PROCEEDINGS B

royalsocietypublishing.org/journal/rspb

Research

Cite this article: Strauss AT, Hite JL, Civitello DJ, Shocket MS, Cáceres CE, Hall SR. 2019 Genotypic variation in parasite avoidance behaviour and other mechanistic, nonlinear components of transmission. *Proc. R. Soc. B* **286**: 20192164.
http://dx.doi.org/10.1098/rspb.2019.2164

Received: 17 September 2019
Accepted: 29 October 2019

Subject Category:
Ecology

Subject Areas:
ecology

Keywords:
transmission, exposure, susceptibility, beta, intraspecific variation, *Daphnia*

Author for correspondence:
Alexander T. Strauss
e-mail: straussa@umn.edu

†Present address: Department of Ecology, Evolution, and Behavior, University of Minnesota, St Paul, MN 55108, USA.
‡Present address: Department of Biological Sciences, University of Nebraska at Lincoln, Lincoln, NE 68588, USA.
¶Present address: Department of Biology, Stanford University, Stanford, CA 94305, USA.

Electronic supplementary material is available online at https://doi.org/10.6084/m9.figshare.c.4728788.

THE ROYAL SOCIETY PUBLISHING

Genotypic variation in parasite avoidance behaviour and other mechanistic, nonlinear components of transmission

Alexander T. Strauss[1,†], Jessica L. Hite[1,‡], David J. Civitello[2], Marta S. Shocket[1,¶], Carla E. Cáceres[3] and Spencer R. Hall[1]

[1]Department of Biology, Indiana University, Bloomington, IN 47401, USA
[2]Department of Biology, Emory University, Atlanta, GA 30322, USA
[3]School of Integrative Biology, University of Illinois at Urbana-Champaign, Urbana, IL 61801, USA

ATS, 0000-0003-0633-8443; DJC, 0000-0001-8394-6288; MSS, 0000-0002-8995-4446

Traditional epidemiological models assume that transmission increases proportionally to the density of parasites. However, empirical data frequently contradict this assumption. General yet mechanistic models can explain why transmission depends nonlinearly on parasite density and thereby identify potential defensive strategies of hosts. For example, hosts could decrease their exposure rates at higher parasite densities (via behavioural avoidance) *or* decrease their per-parasite susceptibility when encountering more parasites (e.g. via stronger immune responses). To illustrate, we fitted mechanistic transmission models to 19 genotypes of *Daphnia dentifera* hosts over gradients of the trophically acquired parasite, *Metschnikowia bicuspidata*. Exposure rate (foraging, F) frequently decreased with parasite density (Z), and per-parasite susceptibility (U) frequently decreased with parasite encounters ($F \times Z$). Consequently, infection rates ($F \times U \times Z$) often peaked at intermediate parasite densities. Moreover, host genotypes varied substantially in these responses. Exposure rates remained constant for some genotypes but decreased sensitively with parasite density for others (up to 78%). Furthermore, genotypes with more sensitive foraging/exposure also foraged faster in the absence of parasites (suggesting 'fast and sensitive' versus 'slow and steady' strategies). These relationships suggest that high densities of parasites can inhibit transmission by decreasing exposure rates and/or per-parasite susceptibility, and identify several intriguing axes for the evolution of host defence.

1. Introduction

Transmission is a critical process for both the ecology and evolution of the disease. In disease ecology, differences in transmission can predict variation in the size of epidemics [1–3]. In turn, differences in transmission among host genotypes can drive host-parasite (co)evolution [4] and the evolution of host resistance [5]. Foundational theory for both disease ecology [6] and evolution [7] assumes that environmental transmission is proportional to the density of parasites in the environment. At first glance, this assumption makes sense: more parasites should increase encounters between hosts and parasites, and more hosts should become infected. Consequently, experiments often estimate a constant per-host, per-parasite transmission coefficient, β. However, models that assume constant per-host, per-parasite transmission often fit data poorly [8–10]. In other words, transmission rarely depends linearly on parasite density [11]. Nonlinear phenomenological functions for β with different densities of parasites, Z (e.g. $\beta(Z) = \beta Z^p$) enable more flexibility [12]. However, they can still misdiagnose the 'shape' of transmission and lack biological meaning [13]. By contrast, general yet mechanistic models can fit data better and enhance biological interpretation [10,13,14]. Further developing such models could help predict both the severity of epidemics and their evolutionary consequences.

Box 1. Terminology.

The transmission of parasites and pathogens can be described with various terms. We summarize definitions employed for each component of transmission here.

Exposure rate (F) is the per-host, per-parasite rate at which a host is exposed to parasites. For directly transmitted parasites, it can also be called 'contact rate', because it is the rate at which a host contacts other hosts. For environmentally transmitted parasites, exposure rate is the rate at which a host 'samples' the environment.

Parasite encounter rate ($F \times Z$) is the rate at which a host encounters parasites. For environmentally transmitted parasites, it is the product of exposure rate (F) and the density of parasites in the environment (Z).

Per-parasite susceptibility (U) is the probability that a host becomes infected, per-parasite encountered. From the parasite's perspective, it can be called 'per-parasite infectivity'.

The transmission coefficient ($\beta = F \times U$) is the per-host, per-parasite risk of infection. It is the product of exposure rate and per-parasite susceptibility.

Infection rate ($\beta \times Z = F \times U \times Z$) is the overall risk of infection per-host. For environmentally transmitted parasites, infection rate is the product of exposure rate (F), per-parasite susceptibility (U) and the density of parasites in the environment (Z).

General mechanistic models that partition transmission into its key components can also delineate defensive strategies of hosts. Transmission occurs when contact with parasites subsequently leads to infection. Therefore, the transmission coefficient can be partitioned into exposure (F)— the rate at which a host is exposed to parasites—and per-parasite susceptibility (U)—the probability of infection per-parasite encountered (box 1) [3,10,13,15]. Importantly, exposure rate could depend nonlinearly on parasite density (Z), and per-parasite susceptibility could depend nonlinearly on the rate at which a host encounters parasites ($F \times Z$). Together, these 'shapes' of exposure and susceptibility suggest several defensive strategies of hosts. For example, uniformly low exposure rate or low per-parasite susceptibility could indicate strong constitutive avoidance or resistance, respectively. Alternatively, many hosts including mammals [16], amphibians [17–19] and insects [20,21] can behaviourally avoid parasites by reducing their exposure rates as the density of parasites increases [22]. This plastic strategy is especially important when exposure occurs via foraging because uniformly slow foraging can be energetically costly [5,23,24]. Similarly, per-parasite susceptibility could decrease with exposure to more parasites if more parasites stimulate stronger immune responses in hosts [25–29]. Thus, potential defensive strategies include constitutively low exposure or susceptibility, plastic exposure that decreases with parasite density, and plastic per-parasite susceptibility that decreases with parasite encounters. The importance of these strategies—and whether different host genotypes use different ones—is less clear.

We addressed these unknowns by fitting mechanistic transmission models to experimental data. We exposed 19 clonal genotypes of water-flea hosts (*Daphnia dentifera*) to a density gradient of its fungal parasite (*Metschnikowia bicuspidata*). Hosts consume fungal spores while non-selectively foraging [10]. We used Akaike information criterion (AIC) to compare models with constant, linear or exponential functions for both exposure (F) and per-parasite susceptibility (U), fitted to each host genotype. The best model indicated exponential changes in exposure with parasite density (Z) *and* exponential changes in per-parasite susceptibility with parasite encounters ($F \times Z$). The combined transmission coefficients ($\beta = F \times U$) declined with parasite density for most hosts, and overall infection rate ($F \times U \times Z$) frequently peaked at intermediate parasite densities. Moreover, these responses varied significantly among host genotypes. Among hosts, per-parasite susceptibility (U) decreased, remained constant or even increased with exposure to more parasites. Foraging/exposure rate (F) remained relatively constant for some genotypes but decreased sensitively with parasites density for others (up to 78%). Finally, more sensitive foragers foraged faster in the absence of parasites. This covariation suggests a spectrum of 'fast and sensitive' to 'slow and steady' foraging strategies. These genotypic differences suggest several intriguing possibilities for the evolution of host defence with cascading ecological implications.

2. Material and methods

(a) Natural history

The host *D. dentifera* is a dominant grazer in midwestern lakes. It frequently suffers epidemics of the virulent fungal parasite *M. bicuspidata* [30]. Hosts are exposed when they inadvertently consume parasite spores while non-selectively filter-feeding for algae [10]. Consequently, the foraging rate on algae can serve as a useful proxy for spore consumption [3,13,24,31]. Infection occurs if spores puncture the host gut and avoid degradation by host haemocytes [32,33]. *Daphnia* hosts can reproduce asexually, and different isoclonal lines (hereafter: genotypes) often vary in key epidemiological traits like exposure (i.e. foraging rate) and per-spore susceptibility [24,34]. Genetic differences among parasite strains do not seem to influence infectivity [35].

(b) Combined foraging and infection assay

We conducted a combined foraging and infection assay for 19 unique host clonal genotypes over a density gradient of parasite spores. All genotypes were chosen from existing cultures isolated from lakes in Michigan or Indiana (USA). Cultures were maintained in high-hardness COMBO (artificial lake water media) and fed high quality, laboratory-cultured algae (2.0 mg mass l^{-1} d^{-1} *Ankistrodesmus falcatus*) for at least three generations to standardize any maternal affects. All parasite spores (approx. six-weeks-old) were reared *in vivo* in a separate host genotype (excluded from the experiment). Spore densities were quantified with a haemocytometer. Because of logistical challenges, the experiment was conducted over three rounds. We standardized all conditions known to affect infectivity of the parasite, including temperature [3], host age [31], algal quality and quantity [10], spore age [36] and host genotype, in which spores were

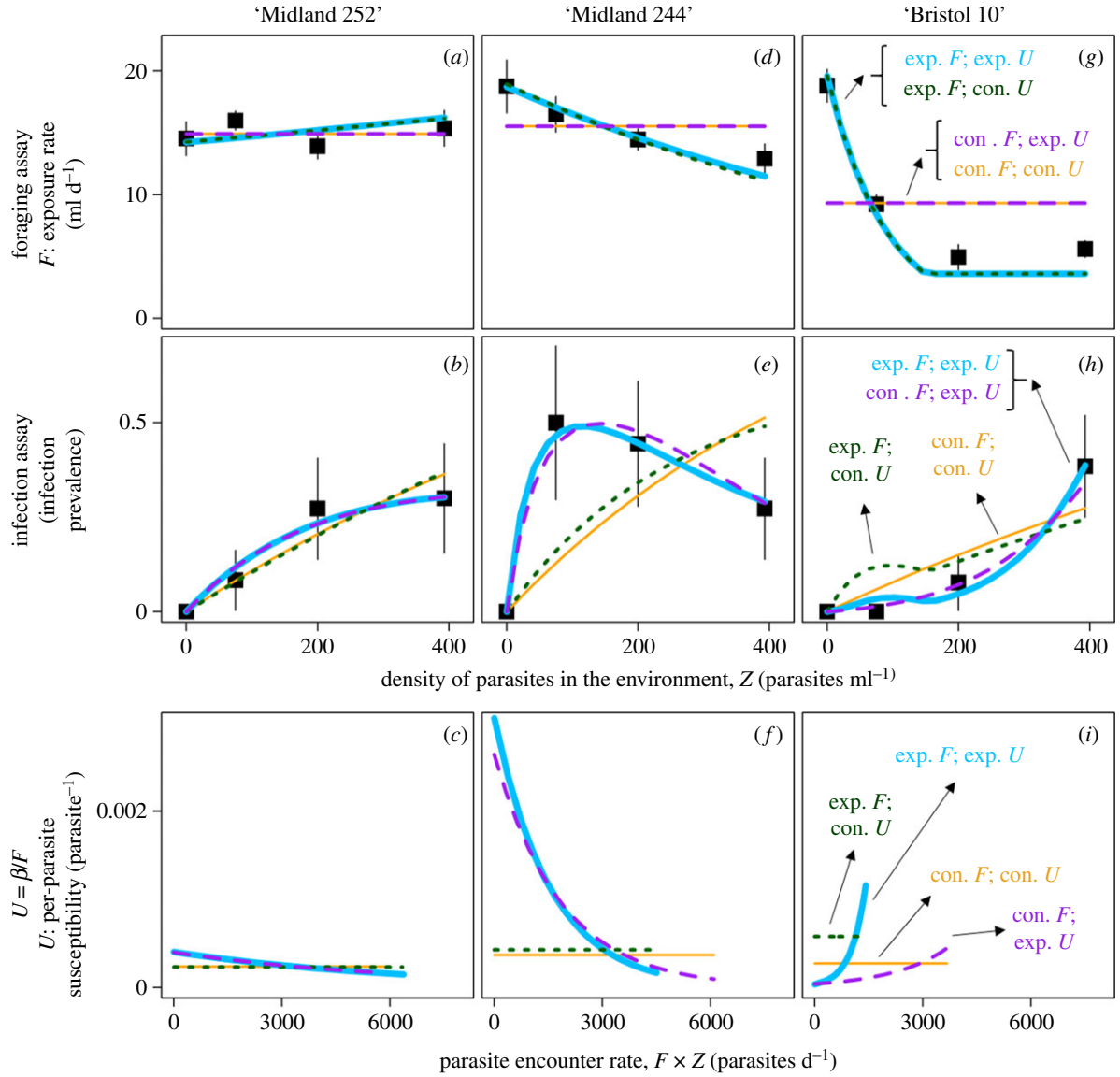

Figure 1. Transmission functions fitted to three example genotypes (columns) showing a range of responses. Points (with standard errors) show data from the assays while lines fit functions to them (table 2). Exposure F is fitted to the foraging assay (*a*,*d*,*g*), transmission coefficients β are fitted to the infection assay (*b*,*e*,*h*), and per-parasite susceptibility U is fitted as β/F (*c*,*f*,*i*). For 'Midland 252' exposure rate does not vary with parasite density (Z), and per-parasite susceptibility does not vary with parasites encountered ($F \times Z$). However, both decrease for 'Midland 244'. 'Bristol 10' (shown from round 2) demonstrates decreasing exposure and increasing per-parasite susceptibility. The best overall model includes exponential functions for both exposure *and* per-parasite susceptibility (thick solid blue; table 2, model A). Also plotted: constant exposure and constant susceptibility (thin solid gold; model I), exponential exposure and constant susceptibility (dotted green; model C), constant exposure and exponential susceptibility (dashed purple; model G). Other combinations not displayed; all genotypes are shown in the electronic supplementary material, figures S2–S4. (Online version in colour.)

reared [35]. To test for round effects, we repeated several genotypes among rounds (19 unique genotypes; 27 genotype-round combinations).

The foraging portion of the assay determined the algae—hence parasites [10]—that were consumed by hosts across the density gradient of parasite spores. We used an algae (*Ankistrodesmus* sp.) that closely resembles the shape (needle-like) and size (40–50 µm long; 3–5 µm wide) of *M. bicuspidata* parasite spores. Because *Daphnia* are non-selective filter-feeders, changes in fluorescence of this algae serve as an accurate proxy for spore consumption (see the electronic supplementary material, figure S1 for experimental verification). We reared cohorts of neonates of each host genotype for five days. Then, individuals were isolated in tubes (volume V = 15 ml) and fed 1.0 mg mass l^{-1} algae (A). Fifteen replicates were inoculated at each of four densities of fungal spores: $Z = 0$, 75, 200 or 393 spores ml^{-1}. This highest density is consistent with large epidemics in nature, as evidenced by the number of spores embedded in host guts in the field versus under these laboratory conditions [37]. Control tubes were treated identically (i.e. contained spores) but omitted hosts. All tubes were inverted every approximately 30 min and kept in the dark for approximately 8 h (t). We then removed hosts and measured *in vivo* fluorescence in control (ungrazed) and experimental (grazed) tubes using a Turner Trilogy Laboratory Fluorometer. We also measured body size (L) of each host with a dissecting microscope and micrometer, because foraging rate is proportional to size [10]. In the first round of the experiment, we only measured fluorescence and body size for the 0 and 393 spores ml^{-1} treatments. Size-specific foraging rates (plotted in figure 1) were calculated as $f = \ln(\text{ungrazed } A/\text{grazed} A)(V/tL^2)$ [38].

The infection portion of the assay determined which individuals became infected. We transferred each host to a fresh 50 ml tube daily and fed it 1.0 mg dry mass l^{-1} d^{-1} algae until death. Infections were diagnosed visually with a dissecting microscope. Individuals that died too early to diagnose were omitted, but this omission did not bias our results (see the electronic

Table 1. Definitions and units of parameters.

parameter	definition	units
Z	density of parasites in the environment	parasites ml^{-1}
F	exposure function over the gradient of parasite density	ml d^{-1}
$\hat{f}$	size-specific exposure (i.e. foraging) rate	ml d^{-1} mm^{-2}
L	length (body size) of the host	mm
$\hat{f}_0$	background size-specific exposure/foraging rate (with 0 parasites)	ml d^{-1} mm^{-2}
α	coefficient of exposure plasticity	ml parasite^{-1} mm^{-2}
$f_{\min}$	minimum exposure (i.e. foraging) rate[a]	ml d^{-1}
U	per-parasite susceptibility function over parasites encountered	parasite^{-1}
u	per-parasite susceptibility	parasite^{-1}
u_0	background per-parasite susceptibility (with 0 parasites)	parasite^{-1}
w	coefficient of susceptibility plasticity	days parasite^{-1}
β	per-host, per-parasite transmission coefficient	ml parasite^{-1} d^{-1}

[a]For all genotypes, $f_{\min} = 3.6$ ml d^{-1}.

supplementary material, appendix). Thus, the combined foraging and infection assay generated three data values for each host: fluorescence of algae, body size and infection status. Next, we fitted mechanistic transmission models to these data to estimate exposure rate and per-parasite susceptibility for each genotype in each round of the experiment.

(c) Model fitting and competition

Our goal is to develop and fit general transmission models with traits that can parametrize dynamical models of disease. Such dynamical models provide powerful tools for delineating feedbacks among hosts, parasites, and resources and predicting drivers and consequences of epidemics [1,13,14]. We also present a more traditional analysis of our data with generalized linear models in the electronic supplementary material, appendix. All transmission models followed a general template that coupled changes in the density of susceptible hosts (S), infected hosts (I), parasite spores (Z) and algal resources (A):

$$\frac{dS}{dt} = -FUSZ, \tag{2.1}$$

$$\frac{dI}{dt} = FUSZ, \tag{2.2}$$

$$\frac{dZ}{dt} = -F(S+I)Z, \tag{2.3}$$

$$\frac{dA}{dt} = -F(S+I)A, \tag{2.4}$$

where F and U describe functions for exposure rate and per-parasite susceptibility, respectively. Thus, $F \times U = \beta$ (box 1), where β is the per-parasite transmission coefficient from traditional epidemiological models [6,7].

We considered constant, linear and exponential variations of exposure (F) over the gradient of parasite density (Z) combined with constant, linear and exponential variations of susceptibility (U) per-parasite encountered (parameters defined in table 1; models lettered A–I in table 2). For models with constant exposure, a single parameter ($\hat{f}$) described the size-corrected foraging rate of each genotype, regardless of parasite density. When exposure could change linearly or exponentially with parasite density, we fitted two exposure parameters: size-corrected background exposure/foraging rate ($\hat{f}_0$; without any parasites) and a size-specific coefficient of exposure plasticity (α). Decreasing exposure rate (negative α) would suggest behavioural avoidance as parasite density increases. A third parameter described a minimum exposure/foraging rate ($f_{\min}$), which could indicate a minimum threshold of feeding needed for host survival (set to a constant for all genotypes based on empirical data: $f_{\min} = 3.6$ ml d^{-1}; see the electronic supplementary material, appendix). In parallel, models with constant susceptibility included a single parameter (u) describing the per-parasite risk of infection. Models where susceptibility could change required two parameters: background per-parasite susceptibility (u_0; without parasites) and a coefficient of susceptibility plasticity (w). Decreasing per-parasite susceptibility (negative w) could reflect immune function that is strongly stimulated by encounters with parasites [26,27,29] or parasite antagonism within hosts [9]. Increasing per-parasite susceptibility (positive w) could reflect easily overwhelmed immune function or parasite synergism [9].

We fitted each transmission model (models A–I; equations (2.1)–(2.4) with each combination of F and U in table 2) using maximum likelihood and the bbmle package in R [39,40]. We fitted different parameters for each genotype in each round of the experiment. Three additional models (J–L) used the best F and U functions but grouped data in strategic combinations. First, we fitted a single set of parameters for each genotype, grouping rounds together if the genotype was repeated, to evaluate the consistency of genotypic responses across rounds (model J). Second, we fitted a single set of parameters for each round, grouping all genotypes together within each round, to evaluate any systematic differences in round (model K). Third, we fitted a single set of five parameters for all data grouped together, across all genotypes and rounds (model L). The likelihood function incorporated fluorescence of experimental and control tubes (i.e. foraging: A), infection status of hosts (I) and body size of each host (L). We simulated numeric solutions to equations (2.1–2.4) using the deSolve package [41]. Starting conditions and time of the simulations mirrored the assay. We assumed normally distributed residuals of the log-transformed fluorescence data [38] and binomially distributed infection data (see the electronic supplementary material, appendix). After fitting, we summed the log-likelihoods across all genotypes to calculate overall AIC scores for each model. We identified the best overall model via model competition [42] and bootstrapped confidence intervals (10 000 bootstraps stratified by levels of parasite density) around its parameters.

The best model indicated exponential exposure (F) and exponential susceptibility (U) fitted independently to each genotype in each round (model A; see Results). We plot its fit for all host genotypes from all rounds of the experiment, contrasted against

Table 2. AIC table for competing models. (exp., exponential; lin., linear; con., constant; $g \times r$, genotype by round combination.)

model ID	transmission function ($\beta = F \times U$)	fit to each	F (ml d^{-1})	U (parasite^{-1})	number of parameters	ΔAIC[a]	Akaike weight, w_{AIC}^{b}
A	exp. F; exp. U	$g \times r$	$\max[\hat{f}_0\ L^2\ \exp(\alpha\ Z\ L^2), f_{min}]$	$u_0\ \exp(w\ Z\ F)$	135	0	0.862
B	exp. F; lin. U	$g \times r$	$\max[\hat{f}_0\ L^2\ \exp(\alpha\ Z\ L^2), f_{min}]$	$u_0\ (1 + w\ Z\ F)$	135	4	0.131
C	exp. F; con. U	$g \times r$	$\max[\hat{f}_0\ L^2\ \exp(\alpha\ Z\ L^2), f_{min}]$	u	108	9	7.5×10^{-3}
D	lin. F; exp. U	$g \times r$	$\max[\hat{f}_0\ L^2\ (1 + \alpha\ Z\ L^2), f_{min}]$	$u_0\ \exp(w\ Z\ F)$	135	22	1.8×10^{-5}
E	lin. F; lin. U	$g \times r$	$\max[\hat{f}_0\ L^2\ (1 + \alpha\ Z\ L^2), f_{min}]$	$u_0\ (1 + w\ Z\ F)$	135	26	2.1×10^{-6}
F	lin. F; con. U	$g \times r$	$\max[\hat{f}_0\ L^2\ (1 + \alpha\ Z\ L^2), f_{min}]$	u	108	33	6.6×10^{-8}
J	exp. F; exp. U	genotype	$\max[\hat{f}_0\ L^2\ \exp(\alpha\ Z\ L^2), f_{min}]$	$u_0\ \exp(w\ Z\ F)$	95	191	2.5×10^{-46}
K	exp. F; exp. U	round	$\max[\hat{f}_0\ L^2\ \exp(\alpha\ Z\ L^2), f_{min}]$	$u_0\ \exp(w\ Z\ F)$	12	405	8.3×10^{-89}
L	exp. F; exp. U	all data	$\max[\hat{f}_0\ L^2\ \exp(\alpha\ Z\ L^2), f_{min}]$	$u_0\ \exp(w\ Z\ F)$	5	539	8.1×10^{-118}
G	con. F; exp. U	$g \times r$	$\hat{f}\ L^2$	$u_0\ \exp(w\ Z\ F)$	108	548	9.4×10^{-120}
H	con. F; lin. U	$g \times r$	$\hat{f}\ L^2$	$u_0\ (1 + w\ Z\ F)$	108	553	7.4×10^{-121}
I	con. F; con. U	$g \times r$	$\hat{f}\ L^2$	u	81	597	2.1×10^{-130}

[a]For the winning model, AIC = −241 and ΔAIC = 0. The other models are sorted by increasing ΔAIC. Generally, ΔAIC > 10 indicates poor model performance.
[b]Akaike weights (w_{AIC}) indicate the probability of a given model being best among those considered.

three poorer models: constant F and constant U (model I); exponential F and constant U (model C); constant F and exponential U (model G; electronic supplementary material, figures S2–S4). These contrasts demonstrate the importance of nonlinearities in both exposure rate *and* per-parasite susceptibility. We highlight three genotypes that illustrate the range of responses (figure 1). We also plot all of the fitted genotypic reaction norms for exposure (F), per-parasite susceptibility (U), the transmission coefficient ($\beta = F \times U$) and overall infection rate ($F \times U \times Z$; figure 2).

(d) Correlations among genotypes

We explored all pairwise correlations of parameters from the best model. We used rank-order Spearman correlation tests, given no *a priori* expectation of linear relationships. Although the best model fitted a separate set of parameters for each genotype in each round (model A), we used one set of parameters per genotype for this analysis to avoid pseudoreplication. Because some genotypes were repeated among rounds, the 19 unique genotypes could be combined in 144 different ways (i.e. using parameters from different combinations of rounds). We report the median observed Spearman correlation of these 144 possible combinations for each relationship ($\widetilde{\text{rho}}_{\text{obs}}$; more details in the electronic supplementary material, appendix). For example, we asked whether foraging in the absence of parasites ($\hat{f}_0$) correlated with the plasticity of exposure/foraging at higher parasite densities (α). Importantly, such correlations could suggest covarying biological traits or statistical properties of the model, because intercepts (e.g. $\hat{f}_0$) and slopes (e.g. α) can covary negatively by chance [43]. Therefore, we randomized the data (fluorescence data sampled with replacement from all genotypes and parasite densities; infections sampled with replacement from all treatments with $Z > 0$), re-fitted the model to 19 arbitrary 'genotypes', and recalculated Spearman correlations 10 000 times. We obtained p-values by asking how frequently the randomized correlations (with median $\widetilde{\text{rho}}_{\text{rand}}$) were more extreme than the observed correlations ($\widetilde{\text{rho}}_{\text{obs}}$). If an observed correlation was more extreme than 95% of randomized correlations ($p < 0.05$), we interpreted it biologically. If it was consistent with the randomized correlations ($p > 0.05$), we interpreted it as a statistical property of the model.

3. Results

(a) Model competition

The winning model required exponential exposure/foraging (F) with parasite density (Z) and exponential per-parasite susceptibility (U) with parasites encountered ($F \times Z$) for each genotype in each round of the experiment (table 2). This model (model A) had a high probability of being best among the models evaluated (Akaike weight, $w_{AIC} = 0.862$). The second ranking model—exponential F and linear U—was worse but still fitted reasonably well (model B; $w_{AIC} = 0.131$). These two models dominated all others. Thus, F needed to be an exponential function of Z, and U also needed to be a function of $F \times Z$ (either exponential or linear). The models assuming exponential exposure but constant susceptibility (the third-ranking model; model C; $w_{AIC} = 7.5 \times 10^{-3}$) and exponential per-parasite susceptibility but constant exposure (the tenth-ranking model; model G; $w_{AIC} = 9.4 \times 10^{-120}$) performed very poorly. The traditional transmission model—constant exposure and constant per-parasite susceptibility—was even worse, despite requiring fewer parameters (81 versus 135 parameters; model I; $w_{AIC} = 2.1 \times 10^{-130}$).

The three grouping models (models J, K and L) indicated that transmission varied among host genotypes and rounds of the experiment. The model that grouped the repeated genotypes across rounds fitted poorly (model J; $w_{AIC} = 2.5 \times 10^{-42}$). Thus, despite the efforts to standardize, genotypes varied in their responses across rounds (graphically depicted in the electronic supplementary material, figure S6). These varied responses could indicate individual heterogeneities [44] but seem beyond the scope of the current analysis.

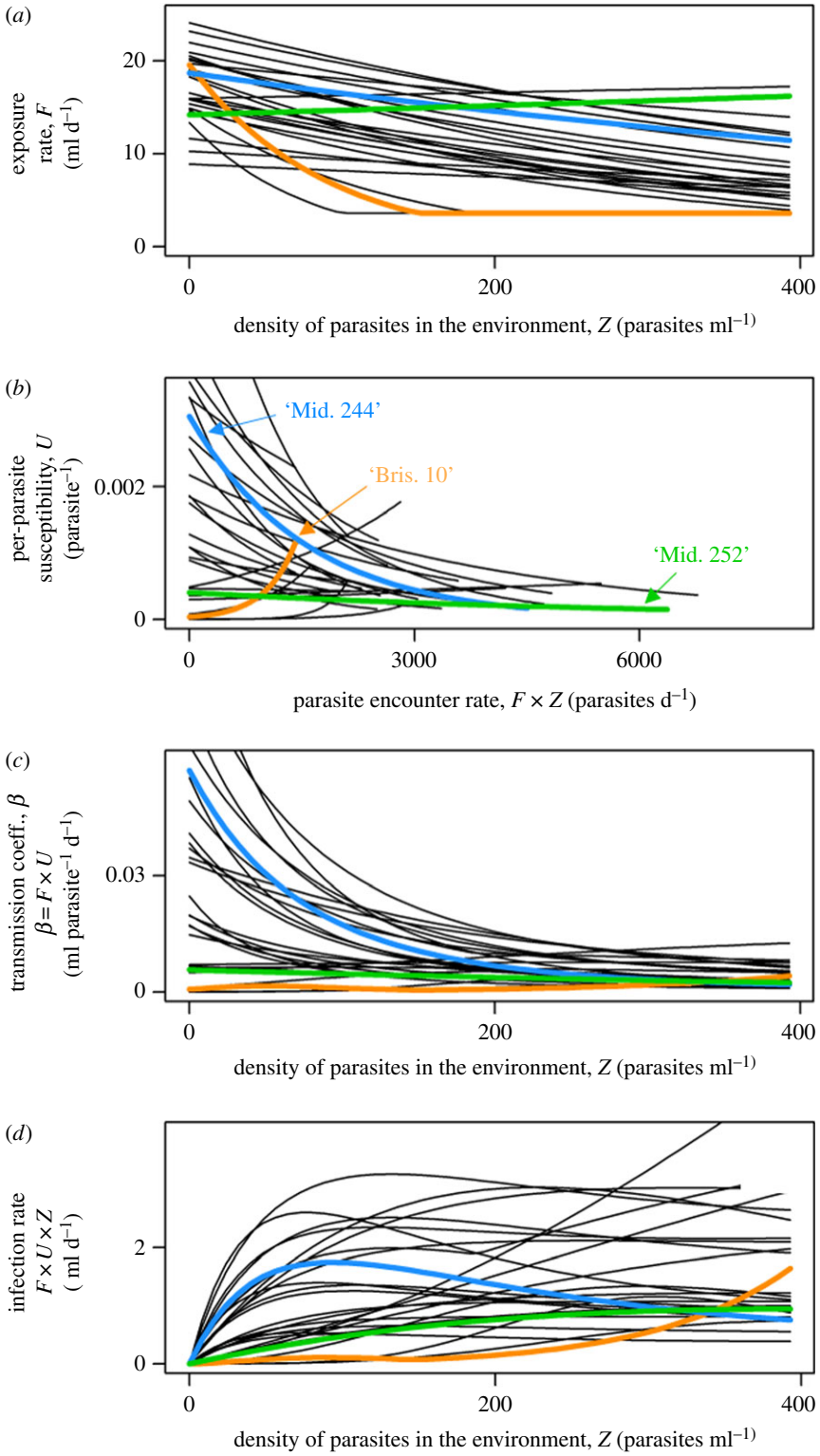

Figure 2. Reaction norms for each component of transmission (defined in box 1). Lines show the best transmission model (table 2, model A) fit for each genotype in each round of the experiment, including the examples in figure 1 (coloured). (*a*) Exposure rate (F) decreases for most host genotypes, with reaction norms frequently crossing over the gradient of parasite density, Z. (*b*) Per-parasite susceptibility (U) increases or decreases—depending on host genotype—with reaction norms also frequently crossing. The range of parasite encounter rates (*x*-axis) differs, given different exposure rates among genotypes (top row). (*c*) Transmission coefficients ($\beta = F \times U$) frequently decrease with Z. Across genotypes, transmission coefficients are variable at low Z but become consistently low at higher Z (because F and/or U decrease). (*d*) Because β decreases with Z, overall infection rates ($F \times U \times Z$) often peak at intermediate Z. Their rank order among genotypes also varies with parasite density. (Online version in colour.)

'Round' by itself explained extremely little variation in the responses of exposure and per-parasite susceptibility to parasite density (model K; $w_{AIC} = 8.3 \times 10^{-89}$). Finally, the model that grouped all data together—even with exponential exposure and susceptibility—was even worse, despite requiring only five parameters (model L; $w_{AIC} = 8.1 \times 10^{-118}$).

(b) Genotypic responses

Genotypes exhibited striking differences in their plastic exposure rates (F) and per-parasite susceptibility (U). Background ($Z = 0$) size-specific exposure rate ($\hat{f}_0$) varied threefold from fast (high $\hat{f}_0$) to slow (low $\hat{f}_0$). For some genotypes, exposure rate remained constant with Z ($\alpha \approx 0$,

'steady'), and for others, it decreased up to 78% at the highest parasite density ($\alpha < 0$, 'sensitive'). Background per-parasite susceptibility (u_0) varied over four orders of magnitude, with some genotypes much more susceptible (high u_0) and others much more resistant (low u_0). Finally, per-parasite susceptibility decreased ($w < 0$), remained constant ($w \approx 0$) or even increased steeply with parasite encounters ($w > 0$).

Three genotypes illustrate this broad range of outcomes (figure 1). First, 'Midland 252' (left column) more or less fits the assumption of constant per-parasite transmission from traditional disease models. Its foraging/exposure rate remains roughly constant ($\alpha \approx 0$: 'steady' foraging) over the gradient of parasite density, Z (figure 1*a*). Its infection prevalence plateaus (figure 1*b*), and its fitted function for per-parasite susceptibility ($U = \beta/F$) also remains relatively constant ($w \approx 0$; figure 1*c*). However, for 'Midland 244' (middle column), exposure rate declines ($\alpha < 0$; 'sensitive' foraging figure 1*d*). Moreover, its infection prevalence suggests a concave-down relationship, peaking at the second-lowest density of parasites (figure 1*e*). Its per-parasite susceptibility also decreases ($w < 0$; figure 1*f*), which contributes to the concave-down shape of infection prevalence (figure 1*e*). 'Bristol 10' (right column; shown from round 2) also illustrates sensitive exposure/foraging ($\alpha < 0$; figure 1*g*). However, its infection prevalence accelerates with more parasites (figure 1*h*). Consequently, its per-parasite susceptibility increases steeply with more parasite encounters ($w > 0$; figure 1*i*). This steeply increasing susceptibility (figure 1*i*) overwhelms the decreasing exposure (figure 1*g*) to yield accelerating prevalence with higher parasite density (figure 1*h*).

Plasticity in exposure and per-parasite susceptibility resulted in highly nonlinear—even non-monotonic—transmission over the gradient of parasite density (figure 2*d*). The genotypic reaction norms for exposure (F, figure 2*a*) and per-parasite susceptibility (U; figure 2*b*) both crossed each other frequently over the gradients of parasite density in the environment (Z) and rate of encountering parasites ($F \times Z$), respectively. In other words, no single genotype consistently demonstrated 'highest' F or 'highest' U. Instead, their rank-order depended on the density of parasites. Transmission coefficients (β, where $\beta = F \times U$) decreased for most genotypes with Z (figure 2*c*). At low parasite densities, transmission coefficients varied substantially. However, transmission coefficients became universally small and less variable at higher parasite densities. Consequently, overall infection rates ($F \times U \times Z$) frequently peaked non-monotonically at intermediate parasite density (figure 2*d*).

(c) Correlations among genotypes

We detected one biological correlation and one statistical relationship between parameters from the best model (figure 3). First, faster foraging in the absence of parasites correlated strongly with more sensitive decreases in exposure rate at higher parasite densities (figure 3*a*). Thus, exposure/foraging varied from slow and steady (small $\hat{f}_0$, α near 0) to fast and sensitive (large $\hat{f}_0$, negative α). This correlation was more extreme than 95% of randomized correlations ($p = 0.038$) and therefore probably reflects covarying biological traits. The two plasticity parameters—plasticity of exposure (α) and susceptibility (w)—were not strongly correlated (figure 3*b*; $p = 0.76$). Background ($Z = 0$) exposure rate and per-parasite susceptibility were also not strongly correlated (figure 3*c*; $p = 0.084$). The intercept (u_0) and slope (w) of per-parasite susceptibility (U) covaried strongly and negatively (figure 3*d*). However, this relationship seems statistical, as most of the randomizations produced similarly strong negative correlations between u_0 and w ($p = 0.74$). Finally, the last two pairs of parameters (α versus u_0 and w versus $\hat{f}_0$) were not strongly correlated (electronic supplementary material, figure S5).

4. Discussion

Ecology and evolution need more powerful, mechanistic models for the transmission of parasites [14]. A traditional simplifying assumption envisions transmission as proportional to parasite density [6,7], yet, models with this assumption often fit data poorly [8–12], and the quest for powerful alternatives remains. General mechanistic models can simultaneously fit better [13] *and* delineate defensive strategies of hosts [21,31]. For example, hosts might decrease their exposure rates at higher densities of parasites (via behavioural avoidance). Other hosts might decrease their per-parasite susceptibility with more parasite encounters (e.g. via immune stimulation). Here, we explored both possibilities by fitting general, mechanistic models to 19 *Daphnia* host genotypes exposed to parasitic *Metschnikowia* spores. Exposure rate (F) frequently declined with parasite density (Z), and per-parasite susceptibility (U) frequently declined with parasite encounters ($F \times Z$). Transmission coefficients ($\beta = F \times U$) declined for most hosts, and overall infection rates ($F \times U \times Z$) often peaked at intermediate densities of the parasite. Critically, these responses varied and covaried dramatically among host genotypes. Exposure rate was relatively constant for some genotypes but decreased sensitively—up to 78%—for others. More sensitive foraging/exposure correlated with faster foraging in the absence of parasites (suggesting 'fast and sensitive' versus 'slow and steady' strategies). Per-parasite susceptibility varied over several orders of magnitude and could increase or decrease with exposure to more parasites. These relationships suggest several intriguing possibilities for the evolution of host defence.

Infection rates often decline with parasite density [11]. Here, mechanistic models showed how exposure and/or susceptibility could cause this decline [14]. The winning model allowed plasticity of both exposure rate *and* per-parasite susceptibility. Given this flexibility, it outperformed all alternatives. How generally applicable is this view of transmission? Exposure rates commonly decrease with higher parasite density. This form of sickness behaviour [22] or parasite avoidance behaviour [45] is common across mammal [16], amphibian [17–19] and insect hosts [20,21]. The 'shape' of per-parasite susceptibility with increasing parasite encounters is less well known (e.g. [9]). Our results could point to within-host dynamics and immune function. For example, exposure to parasites can stimulate rapid immune function in invertebrates [25,46–48], and intestinal parasites can stimulate immune function in mammals [28,29]. However, rapid immune responses are rarely delineated across gradients of parasite encounter rates (but see [26,27,49]). Thus, plasticity in exposure with parasite density (here, α) arises commonly among diverse hosts, but plasticity in per-parasite susceptibility (w) remains an open area of research.

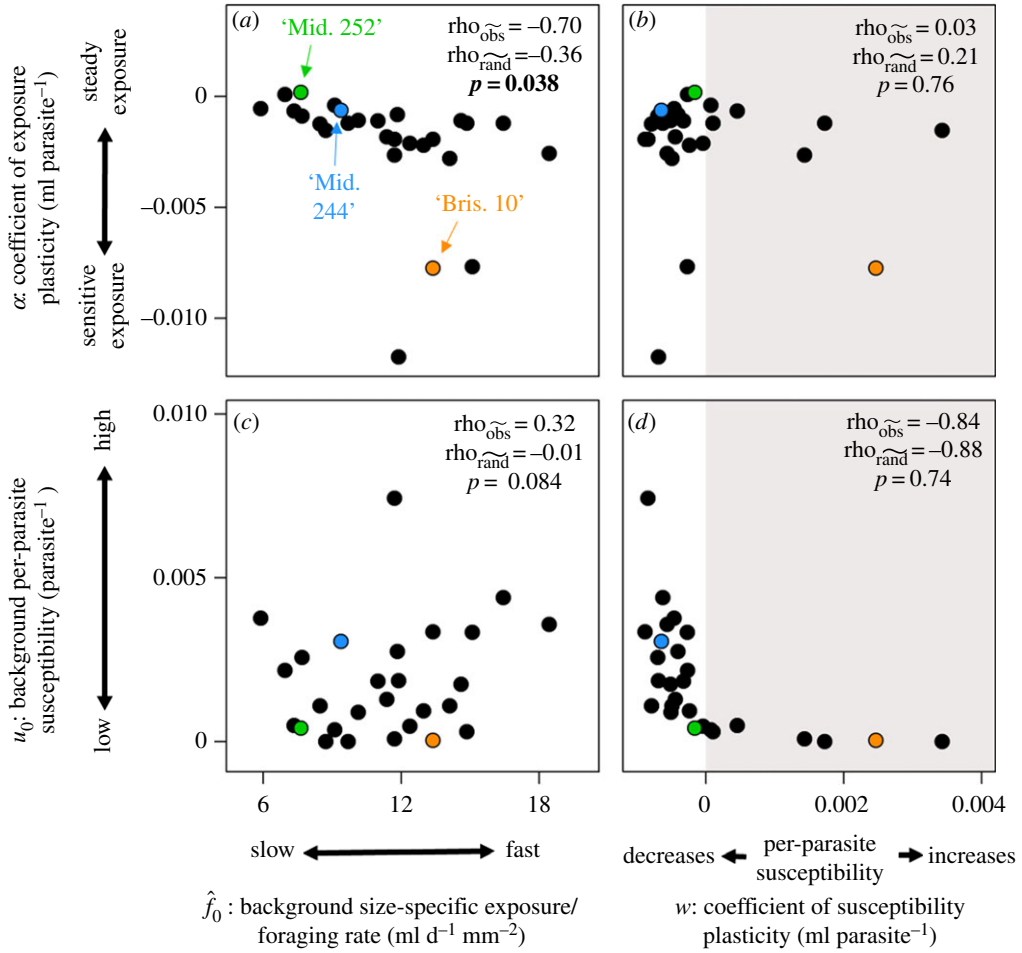

Figure 3. Correlations between parameters from the winning model (model A). *p*-values indicate the proportion of randomized Spearman correlations (with median rho $\widetilde{\text{rho}}_{\text{rand}}$) that are more extreme than the observed correlation rho_{obs}). (*a*) The two exposure parameters significantly vary from fast (large $\hat{f}_0$) and sensitive (negative α) to slow (small $\hat{f}_0$) and steady (α near 0). (*b*) Plasticity of exposure (α) and susceptibility (w) are not correlated. (*c*) Background exposure/foraging rate ($\hat{f}_0$) and background per-parasite susceptibility (u_0) are also not correlated. (*d*) The two susceptibility parameters (w, u_0) covary strongly and negatively, but this covariance arises as a statistical side effect of fitting intercepts (u_0) and slopes (w) for per-parasite susceptibility (U; $p > 0.05$). The last two parameter combinations (α versus u_0 and w versus $\hat{f}_0$) are not correlated (electronic supplementary material, figure S5). Note: parameters are plotted for all genotypes in all rounds, but the correlation statistics account for pseudoreplication by including only a single parameter set per genotype; the observed correlation rho_{obs} is the median among all combinations of the 19 genotypes. (Online version in colour.)

Covariation in foraging/exposure (F) among genotypes suggested a spectrum of 'fast and sensitive' to 'slow and steady' foraging strategies. Depending on host genotype, exposure rate declined up to 78% with parasite density or remained relatively constant. Plasticity of exposure also varies among family lines of gypsy moths, with only some families lowering their exposure rates at higher densities of parasites [21]. Thus, parasite avoidance behaviour may be a general, heritable trait that could undergo natural selection during epidemics. In addition to varying among genotypes here, exposure plasticity (α) also significantly covaried with background foraging/exposure rate ($\hat{f}_0$). The 'fast and sensitive' strategy could allow hosts to acquire resources when parasites are rare but mitigate exposure if parasites become too common. However, the evolutionary coexistence of 'slow and steady' foraging suggests that detection of parasites may be costly (e.g. risk of infection before detection). Delineating the costs and benefits of these strategies would probably require a closer inspection of the impacts of resources and infection on host fitness [22,50]. Such evolution could also have cascading ecological consequences [45], especially when exposure is linked to foraging. For example, if host populations evolve fast and sensitive foraging/exposure, then high densities of parasites could release resources from top-down control by strongly reducing hosts' *per capita* consumption of resources: a trait-mediated trophic cascade driven by parasites. This intersection of evolution, ecology and behaviour promises exciting frontiers.

Among genotypes, per-parasite susceptibility (U) declined, remained constant, or even increased with parasite encounters. These shapes might reflect multiple lines of defence in host immune function. For example, background per-parasite susceptibility (u_0) could reflect constitutive defence, whereas susceptibility plasticity (w) could reflect an induced defence [29,32,33]. Here, low background susceptibility (u_0) was associated with steep increases in per-parasite susceptibility with more parasite encounters (positive w). This correlation was probably statistical, but it is also consistent with a trade-off between constitutive and induced defence [49,51]. More specialized data, e.g. host immune function across gradients of parasite encounter rates [26,27,37], may be necessary to understand such genotypic differences and parametrize even more mechanistic transmission models that include immune function. Nevertheless, if exposure is linked to foraging [1,10,23] and immune function is energetically costly [51,52], these

correlations paint a complicated picture for the evolution of host defence [22]. If parasite avoidance behaviour reduces resource acquisition, resource limitation might starve immune function. Alternatively, stronger immune function fuelled by more resources could obviate the need to avoid parasites. These fascinating potential trade-offs emerge at the intersection of consumer-resource dynamics, behavioural ecology and eco-immunology [22].

Predicting evolutionary changes in host populations during epidemics remains challenging, especially when exposure is linked to foraging [5,53]. For example, small epidemics can select for *increases* in transmission coefficients ($\beta = F \times U$) if such adaptations allow hosts to acquire more resources (larger F) [5]. Here, transmission ($F \times U \times Z$) peaked for different genotypes at different densities of the parasite. Thus, parasite-mediated selection could vary over the course of epidemics, as the density of parasites in the environment waxes and wanes. Moreover, the results here suggest a broad range of defensive strategies that could evolve, including plastic exposure rate (F) and per-parasite susceptibility (U). Natural selection among these strategies should depend on trade-offs linking resource acquisition, detection of parasites and immune function [5,22,31,50,54]. Fascinating eco-evolutionary feedbacks seem likely to emerge, because all of these costs and benefits depend on the density of parasites in the environment, and the density of parasites should likewise depend on traits of evolving host populations. It should be noted that the genotypic responses here arose from individually exposed hosts. It remains to be seen whether such trait variation scales to population, where evolution occurs (but see [2,53]). Other dynamics could also arise at the population level, including feedbacks that hinge on the density of hosts. For example, high host density can decrease per-host infection rates [13], and virulent infections can depress host density [6]. Dynamical models—parametrized with the defensive strategies suggested here—will be required to explore such complex eco-evolutionary dynamics.

Exposure rates that vary plastically with parasite density and per-parasite susceptibility that varies plastically with parasite encounters matter for both ecology and evolution. Here, high densities of parasites actually inhibited transmission through decreases in both components of the transmission. Both of these mechanisms probably constrain the size of epidemics. Moreover, host genotypes differed strikingly in their responses, suggesting several intriguing directions and constraints for the evolution of host defence. We hope that these mechanistic insights into transmission across gradients of parasite density will help advance theory for both the ecology and evolution of disease.

Data accessibility. All data and code are publicly available on the Dryad Digital Repository: https://doi.org/10.5061/dryad.hhmgqnkcf [55].

Authors' contributions. A.T.S., S.R.H. and C.E.C. designed the study. A.T.S., J.L.H., S.R.H. and M.S.S. collected data. A.T.S. implemented the model fitting and competition, with assistance from D.J.C.; A.T.S. wrote the first draft of the manuscript, and all authors contributed to revisions.

Competing interests. We declare we have no competing interests.

Funding. This work was supported by NSF DEB (grant nos 1120316, 1353749 and 1406846). A.T.S. was supported by the NSF GRFP.

Acknowledgements. O. Schmidt assisted with the foraging and infection assays. K. Shaw helped develop the complementary model presented in the electronic supplementary material, appendix.

References

1. Dwyer G, Elkinton JS. 1993 Using simple models to predict virus epizootics in gypsy-moth populations. *J. Anim. Ecol.* **62**, 1–11. (doi:10.2307/5477)
2. Strauss AT, Bowling AM, Duffy MA, Cáceres CE, Hall SR. 2018 Linking host traits, interactions with competitors and disease: mechanistic foundations for disease dilution. *Funct. Ecol.* **32**, 1271–1279. (doi:10.1111/1365-2435.13066)
3. Shocket MS, Strauss AT, Hite JL, Šljivar M, Civitello DJ, Duffy MA, Cáceres CE, Hall SR. 2018 Temperature drives epidemics in a zooplankton-fungus disease system: a trait-driven approach points to transmission via host foraging. *Am. Nat.* **191**, 435–451. (doi:10.1086/696096)
4. Lively CM, Dybdahl MF. 2000 Parasite adaptation to locally common host genotypes. *Nature* **405**, 679–681. (doi:10.1038/35015069)
5. Duffy MA, Ochs JH, Penczykowski RM, Civitello DJ, Klausmeier CA, Hall SR. 2012 Ecological context influences epidemic size and parasite-driven evolution. *Science* **335**, 1636–1638. (doi:10.1126/science.1215429)
6. Anderson RM, May RM. 1981 The population dynamics of micro-parasites and their invertebrate hosts. *Phil. Trans. R. Soc. Lond. B* **291**, 451–524. (doi:10.1098/rstb.1981.0005)
7. May RM, Anderson RM. 1983 Epidemiology and genetics in the coevolution of parasites and hosts. *Proc. R. Soc. Lond. B* **219**, 1216. (doi:10.1098/rspb.1983.0075)
8. D'Amico V, Elkinton JS, Dwyer G, Burand JP, Buonaccorsi JP. 1996 Virus transmission in gypsy moths is not a simple mass action process. *Ecology* **77**, 201–206. (doi:10.2307/2265669)
9. Ben-Ami F, Regoes RR, Ebert D. 2008 A quantitative test of the relationship between parasite dose and infection probability across different host-parasite combinations. *Proc. R. Soc. B* **275**, 853–859. (doi:10.1098/rspb.2007.1544)
10. Hall SR, Sivars-Becker L, Becker C, Duffy MA, Tessier AJ, Cáceres CE. 2007 Eating yourself sick: transmission of disease as a function of foraging ecology. *Ecol. Lett.* **10**, 207–218. (doi:10.1111/j.1461-0248.2007.01011.x)
11. Fenton A, Fairbairn JP, Norman R, Hudson PJ. 2002 Parasite transmission: reconciling theory and reality. *J. Anim. Ecol.* **71**, 893–905. (doi:10.1046/j.1365-2656.2002.00656.x)
12. Hochberg ME. 1991 Nonlinear transmission rates and the dynamics of infectious disease. *J. Theor. Biol.* **153**, 301–321. (doi:10.1016/S0022-5193(05)80572-7)
13. Civitello DJ, Pearsall S, Duffy MA, Hall SR. 2013 Parasite consumption and host interference can inhibit disease spread in dense populations. *Ecol. Lett.* **16**, 626–634. (doi:10.1111/ele.12089)
14. McCallum H *et al*. 2017 Breaking beta: deconstructing the parasite transmission function. *Phil. Trans. R. Soc. B* **372**, 20160084. (doi:10.1098/rstb.2016.0084)
15. Civitello DJ, Rohr JR. 2014 Disentangling the effects of exposure and susceptibility on transmission of the zoonotic parasite *Schistosoma mansoni*. *J. Anim. Ecol.* **83**, 1379–1386. (doi:10.1111/1365-2656.12222)
16. Weinstein SB, Buck JC, Young HS. 2018 A landscape of disgust. *Science* **359**, 1213–1214. (doi:10.1126/science.aas8694)
17. Koprivnikar J, Redfern JC, Mazier HL. 2014 Variation in anti-parasite behaviour and infection among larval amphibian species. *Oecologia* **174**, 1179–1185. (doi:10.1007/s00442-013-2857-7)
18. Marino JA. 2016 Interspecific variation in larval anuran anti-parasite behavior: a test of the adaptive plasticity hypothesis. *Evol. Ecol.* **30**, 635–648. (doi:10.1007/s10682-016-9831-x)
19. Sears BF, Snyder PW, Rohr JR. 2015 Host life history and host-parasite syntopy predict behavioural

resistance and tolerance of parasites. *J. Anim. Ecol.* **84**, 625–636. (doi:10.1111/1365-2656.12333)

20. Eakin L, Wang M, Dwyer G. 2015 The effects of the avoidance of infectious hosts on infection risk in an insect-pathogen interaction. *Am. Nat.* **185**, 100–112. (doi:10.1086/678989)
21. Parker BJ, Elderd BD, Dwyer G. 2010 Host behaviour and exposure risk in an insect–pathogen interaction. *J. Anim. Ecol.* **79**, 863–870. (doi:10.1111/j.1365-2656.2010.01690.x)
22. Hite JL, Pfenning AC, Cressler CE. In press. Starving the enemy? Feeding behavior shapes host-parasite interactions. *Trends Ecol. Evol.*
23. Hutchings MR, Judge J, Gordon IJ, Athanasiadou S, Kyriazakis I. 2006 Use of trade-off theory to advance understanding of herbivore–parasite interactions. *Mamm. Rev.* **36**, 1–16. (doi:10.1111/j.1365-2907.2006.00080.x)
24. Hall SR, Becker CR, Duffy MA, Cáceres CE. 2010 Variation in resource acquisition and use among host clones creates key epidemiological trade-offs. *Am. Nat.* **176**, 557–565. (doi:10.1086/656523)
25. Freitak D, Wheat CW, Heckel DG, Vogel H. 2007 Immune system responses and fitness costs associated with consumption of bacteria in larvae of *Trichoplusia ni*. *BMC Biol.* **5**, 56. (doi:10.1186/1741-7007-5-56)
26. Auld S, Edel KH, Little TJ. 2012 The cellular immune response of *Daphnia magna* under host-parasite genetic variation and variation in initial dose. *Evolution* **66**, 3287–3293. (doi:10.1111/j.1558-5646.2012.01671.x)
27. Tate AT, Graham AL. 2017 Dissecting the contributions of time and microbe density to variation in immune gene expression. *Proc. R. Soc. B* **284**, 20170727. (doi:10.1098/rspb.2017.0727)
28. Keymer A. 1982 Density-dependent mechanisms in the regulation of intestinal helminth populations. *Parasitology* **84**, 573–587. (doi:10.1017/S0031182000052847)
29. Bleay C, Wilkes CP, Paterson S, Viney ME. 2007 Density-dependent immune responses against the gastrointestinal nematode *Strongyloides ratti*. *Int. J. Parasit.* **37**, 1501–1509. (doi:10.1016/j.ijpara.2007.04.023)
30. Strauss AT, Shocket MS, Civitello DJ, Hite JL, Penczykowski RM, Duffy MA, Cáceres CE, Hall SR. 2016 Habitat, predators, and hosts regulate disease in *Daphnia* through direct and indirect pathways. *Ecol. Monogr.* **86**, 393–411. (doi:10.1002/ecm.1222)
31. Hite JL, Penczykowski RM, Shocket MS, Griebel KA, Strauss AT, Duffy MA, Cáceres CE, Hall SR. 2017 Allocation, not male resistance, increases male frequency during epidemics: a case study in facultatively sexual hosts. *Ecology* **98**, 2773–2783. (doi:10.1002/ecy.1976)
32. Metschnikoff E. 1884 A disease of *Daphnia* caused by a yeast. A contribution to the theory of phagocytes as agents for attack on disease-causing organisms. *Arciv. Path. Anat. Phys. Klin. Med.* **96**, 177–195.
33. Stewart MTE, Cáceres CE. 2018 Within-host complexity of a plankton-parasite interaction. *Ecology* **99**, 2864–2867. (doi:10.1002/ecy.2483)
34. Auld S, Penczykowski RM, Ochs JH, Grippi DC, Hall SR, Duffy MA. 2013 Variation in costs of parasite resistance among natural host populations. *J. Evol. Biol.* **26**, 2479–2486. (doi:10.1111/jeb.12243)
35. Searle CL, Ochs JH, Caceres CE, Chiang SL, Gerardo NM, Hall SR, Duffy MA. 2015 Plasticity, not genetic variation, drives infection success of a fungal parasite. *Parasitology* **142**, 839–848. (doi:10.1017/S0031182015000013)
36. Duffy MA, Hunsberger KK. 2019 Infectivity is influenced by parasite spore age and exposure to freezing: do shallow waters provide *Daphnia* a refuge from some parasites? *J. Plankton Res.* **41**, 12–16. (doi:10.1093/plankt/fby046)
37. Stewart MTE. 2019 Variable immunity and its consequences for parasite dynamics. Doctoral Dissertation, University of Illinois Champaign, IL, USA.
38. Sarnelle O, Wilson AE. 2008 Type III functional response in *Daphnia*. *Ecology* **89**, 1723–1732. (doi:10.1890/07-0935.1)
39. Bolker BM. 2008 *Ecological models and data in R*. Princeton, NJ: Princeton University Press.
40. R Core Team. 2017 *R: a language and environment for statistical computing*. Vienna, Austria: R Foundation for Statistical Computing.
41. Soetaert K, Petzoldt T, Setzer RW. 2010 Solving differential equations in R: package deSolve. *J. Stat. Softw.* **33**, 1–25.
42. Burnham KP, Anderson DR. 2002 *Model selection and inference: a practical information-theoretic approach*. New York, NY: Springer.
43. Schielzeth H. 2010 Simple means to improve the interpretability of regression coefficients. *Methods Ecol. Evol.* **1**, 103–113. (doi:10.1111/j.2041-210X.2010.00012.x)
44. Cressler CE, Bengtson S, Nelson WA. 2017 Unexpected nongenetic individual heterogeneity and trait covariance in *Daphnia* and its consequences for ecological and evolutionary dynamics. *Am. Nat.* **190**, E13–E27. (doi:10.1086/691779)
45. Buck JC, Weinstein SB, Young HS. 2018 Ecological and evolutionary consequences of parasite avoidance. *Trends Ecol. Evol.* **33**, 619–632. (doi:10.1016/j.tree.2018.05.001)
46. Lindsey E, Altizer S. 2009 Sex differences in immune defenses and response to parasitism in monarch butterflies. *Evol. Ecol.* **23**, 607–620. (doi:10.1007/s10682-008-9258-0)
47. Moret Y, Siva-Jothy MT. 2003 Adaptive innate immunity? Responsive-mode prophylaxis in the mealworm beetle, *Tenebrio molitor*. *Proc. R. Soc. B* **270**, 2475–2480. (doi:10.1098/rspb.2003.2511)
48. Pham LN, Dionne MS, Shirasu-Hiza M, Schneider DS. 2007 A specific primed immune response in *Drosophila* is dependent on phagocytes. *PLoS Pathog.* **3**, 8. (doi:10.1371/journal.ppat.0030008)
49. Graham AL, Shuker DM, Pollitt LC, Auld S, Wilson AJ, Little TJ. 2011 Fitness consequences of immune responses: strengthening the empirical framework for ecoimmunology. *Funct. Ecol.* **25**, 5–17. (doi:10.1111/j.1365-2435.2010.01777.x)
50. Cressler CE, King AA, Werner EE. 2010 Interactions between behavioral and life-history trade-offs in the evolution of integrated predator-defense plasticity. *Am. Nat.* **176**, 276–288. (doi:10.1086/655425)
51. Diamond SE, Kingsolver JG. 2011 Host plant quality, selection history and trade-offs shape the immune responses of *Manduca sexta*. *Proc. R. Soc. B* **278**, 289–297. (doi:10.1098/rspb.2010.1137)
52. Konig C, Schmidhempel P. 1995 Foraging activity and immunocompetence in workers of the bumble bee, *Bombus terrestris* L. *Proc. R. Soc. Lond. B* **260**, 225–227. (doi:10.1098/rspb.1995.0084)
53. Strauss AT, Hite JL, Shocket MS, Cáceres CE, Duffy MA, Hall SR. 2017 Rapid evolution rescues hosts from competition and disease but—despite a dilution effect—increases the density of infected hosts. *Proc. R. Soc. B* **284**, 20171970. (doi:10.1098/rspb.2017.1970)
54. Tate AT. 2016 The interaction of immune priming with different modes of disease transmission. *Front. Microbiol.* **7**, 1102.
55. Strauss AT, Hite JL, Civitello DJ, Shocket MS, Cáceres CE, Hall SR. 2019 Data from: Genotypic variation in parasite avoidance behaviour and other mechanistic, nonlinear components of transmission. Dryad Digital Repository. (https://doi.org/10.5061/dryad.hhmgqnkcf)